Theory of mixed-state effect on NMR relaxation measurements in iron pnictide superconductors

Yi Gao,[1,2] Jian-Xin Zhu,[3] C. S. Ting,[1] and Wu-Pei Su[1]

[1]*Department of Physics and Texas Center for Superconductivity, University of Houston, Houston, Texas, 77204, USA*
[2]*Department of Physics and Institute of Theoretical Physics, Nanjing Normal University, Nanjing, Jiangsu, 210046, China*
[3]*Theoretical Division, Los Alamos National Laboratory, Los Alamos, New Mexico, 87545, USA*

Based on a phenomenological model with $s_\pm$ or s-wave pairing symmetry, the spatially resolved nuclear magnetic resonance (NMR) relaxation rate in the iron pnictides is investigated by solving Bogoliubov-de Gennes equations. Taking into account the presence of a magnetic field, our result for the $s\pm$ pairing is in qualitative agreement with recent NMR experiments, while for the s-wave pairing, a coherence peak shows up right below T_c in apparent contradiction with experimental observations, thus excluding the s-wave pairing. We also propose that the spin-lattice relaxation rate (SLRR) should follow an exponential relation when the temperature is lowered below $T/T_c \approx 0.1$ down to 0.01. It is noted that the SLRR cannot be entirely determined by the local density of states; the mixed-state effect and multiorbital physics must be considered.

I. INTRODUCTION

The iron pnictide superconductors have attracted much attention since their recent discovery.[1] One of the fascinating issues surrounding these materials is the symmetry and structure of the superconducting (SC) gap. Theoretically it was suggested that the pairing may be established via interpocket scattering of electrons between the hole and electron pockets (around the Γ and M points, respectively), leading to the so-called extended s-wave or $s_\pm$ pairing symmetry ($\Delta_{\mathbf{k}} \sim \cos k_x + \cos k_y$ defined in the 2Fe/cell Brillouin zone).[2] Experimentally, the results on the pairing symmetry remain highly controversial. For example, in $Ba_{0.6}K_{0.4}Fe_2As_2$, an optimally hole-doped pnictide superconductor,[3] the SC gaps measured by angle resolved photoemission spectroscopy (ARPES) can be approximately fitted by $|\Delta_{\mathbf{k}}| \sim |\cos k_x + \cos k_y|$, with no node and almost isotropic gaps on all the Fermi surfaces (FSs),[4] indicating the possible pairing symmetry to be $s_\pm$ or s-wave. However, the spin-lattice relaxation rate (SLRR) T_1^{-1} in the iron pnictides measured by nuclear magnetic resonance (NMR) universally does not exhibit a coherence peak below T_c and has a power-law behavior for $0.1 < T/T_c < 0.5$ (i.e., $T_1^{-1} \sim T^n$) with n varying from 3–5 among different materials,[5,6] which is seemingly the evidence for unconventional superconductivity with line nodes.

To explain the discrepancy of the pairing symmetry inferred from different experimental techniques, several theoretical groups suggested that the $s_\pm$ pairing could explain the lack of a coherence peak and the low-temperature power-law behavior in the SLRR by introducing impurity scattering.[7] However, the impurity concentration and the scattering strength need fine tuning. Therefore, in view of the diversity of the iron pnictide compounds, this theory may lack universality. Another group suggested that a fully gapped $s_\pm$ pairing with the strong anisotropy of the SC gaps on the electron pockets could also explain the NMR results.[8] But the SC gaps measured by ARPES are almost isotropic[4] with only minor variations on all the FSs, thus posing a great challenge to the latter explanation. Furthermore, no magnetic field is considered in all these theoretical studies, while in NMR experiments conducted in the iron pnictides, a magnetic field at around 6–12 Tesla is always present, thus the contributions from vortices are included in their data.[5,6] Usually, T_1 is measured by selecting the resonance frequency (RF) at the most intensive signal in the resonance spectrum (RS). However, the RS reflects information on the internal magnetic field distribution of the vortex lattice.[9] By choosing the RF, we can specify the position to detect the NMR signal. The signal at the maximum (minimum) cutoff comes from the vortex core center (the farthest) site. The signal at the logarithmic singularity of the RS comes from the saddle point of the field. By studying the position dependence of T_1 around vortices through the RF dependence, we can clarify the detail of the vortex contribution in NMR experiments and this idea has been studied both theoretically[10] and experimentally[11] in high-T_c cuprates. It can help us in the analysis of the standard procedure of extracting the gap symmetry.

In order to explain the seemingly contradictory experimental observations, in this work we adopt a phenomenological model with $s_\pm$ pairing symmetry to study the vortex effect on NMR relaxation measurements in the iron pnictides from the SLRR. For comparison, the problem is also studied for s-wave pairing. We focus on the hole-doped 122 system $Ba_{1-x}K_xFe_2As_2$ for two reasons: First, large homogeneous single crystals are available; second, K is not doped into the Fe layer, making it relatively clean compared to the electron-doped $Ba(Fe_{1-x}Co_x)_2As_2$. Thus the data are less affected by impurity scattering and should more accurately reveal the intrinsic properties.

II. METHOD

We begin with an effective two-orbital model on a two-dimensional lattice[12] with a phenomenological form for the intraorbital pairing terms. The Hamiltonian is

$$H = -\sum_{ij,\alpha\beta,\sigma} (t'_{ij,\alpha\beta} + \mu\delta_{ij}\delta_{\alpha\beta})c^\dagger_{i\alpha\sigma}c_{j\beta\sigma}$$
$$+ \sum_{ij,\alpha\beta}(\Delta_{ij,\alpha\beta}c^\dagger_{i\alpha\uparrow}c^\dagger_{j\beta\downarrow} + \text{H.c.}). \tag{1}$$

Here i/j and $\alpha/\beta = 1,2$ are the site and orbital indices, respectively. σ represents the spin and μ is the chemical potential. $\Delta_{ij,\alpha\beta} = \frac{V_{ij}\delta_{\alpha\beta}}{2}(\langle c_{j\beta\downarrow}c_{i\alpha\uparrow}\rangle - \langle c_{j\beta\uparrow}c_{i\alpha\downarrow}\rangle)$ is the intraorbital spin singlet bond order parameter, where V_{ij} is the onsite $[i = j]$ or next-nearest-neighbor (NNN) $[i = j \pm (\hat{x} \pm \hat{y})]$ attraction that we choose to achieve the s-wave or $s_\pm$ pairing symmetry, respectively. The reason we adopt this model is its ability[12] to qualitatively account for the doping evolution of the FSs as observed by ARPES[13] on the K- and Co-doped 122 family of the iron pnictides. More importantly, based on this model, the existence of the negative-energy (NE) in-gap peak in the local density of states (LDOS) at the vortex core center observed by scanning tunneling spectroscopy (STM)[14] has been successfully explained,[15] all justifying the validity of this model. In the presence of a magnetic field B perpendicular to the plane, the hopping integral can be expressed as $t'_{ij,\alpha\beta} = t_{ij,\alpha\beta}\exp[i\frac{\pi}{\Phi_0}\int_j^i \mathbf{A}(\mathbf{r}) \cdot d\mathbf{r}]$, where $\Phi_0 = hc/2e$ is the SC flux quantum, and $\mathbf{A} = (-By,0,0)$ is the vector potential in the Landau gauge. Following Ref. 12, we have

$$t_{ij,\alpha\beta} = \begin{cases} t_1 & \alpha = \beta, i = j \pm \hat{x}(\hat{y}), \\ \frac{1+(-1)^j}{2}t_2 + \frac{1-(-1)^j}{2}t_3 & \alpha = \beta, i = j \pm (\hat{x} + \hat{y}), \\ \frac{1+(-1)^j}{2}t_3 + \frac{1-(-1)^j}{2}t_2 & \alpha = \beta, i = j \pm (\hat{x} - \hat{y}), \\ t_4 & \alpha \neq \beta, i = j \pm (\hat{x} \pm \hat{y}), \\ 0 & \text{otherwise.} \end{cases}$$

(2)

Eq. (1) can be diagonalized by solving the Bogoliubov-de Gennes equations

$$H = C^\dagger MC,$$
$$C^\dagger = (\ldots, c_{j1\uparrow}^\dagger, c_{j1\downarrow}, c_{j2\uparrow}^\dagger, c_{j2\downarrow}, \ldots),$$

(3)

subject to the self-consistency conditions

$$\Delta_{ij,\alpha\beta} = \frac{V_{ij}}{2}\delta_{\alpha\beta}\sum_{k=1}^L (Q_{mk}^*Q_{nk} + Q_{n+1k}^*Q_{m-1k})f(E_k). \quad (4)$$

Here $L = 4N_xN_y$, with N_x/N_y being the number of lattice sites along the $\hat{x}/\hat{y}$ direction of the 2D lattice.

$$m = 4(j_y + N_y j_x) + 2\beta,$$
$$n = 4(i_y + N_y i_x) + 2\alpha - 1,$$

(5)

and Q is a unitary matrix that satisfies $(Q^\dagger MQ)_{kp} = \delta_{kp}E_k$. Here we used $i = (i_x, i_y)$ and $j = (j_x, j_y)$, with $i_x, j_x = 0, 1, \ldots, N_x - 1$ and $i_y, j_y = 0, 1, \ldots, N_y - 1$. The chemical potential μ is determined by the doping concentration x.

The $s_\pm$ order parameter at site j is

$$\Delta'_{j\beta} = \frac{1}{4}\sum_{i=j\pm(\hat{x}\pm\hat{y})}\Delta'_{ij,\beta\beta}, \quad (6)$$

where $\Delta'_{ij,\beta\beta} = \Delta_{ij,\beta\beta}\exp[i\frac{\pi}{\Phi_0}\int_j^{(i+j)/2}\mathbf{A}(\mathbf{r})\cdot d\mathbf{r}]$.[10]

The s-wave order parameter is $\Delta_{jj,\beta\beta}$ and the LDOS is given by

$$\rho_i(\omega) = \sum_{k=1}^L\sum_\alpha [|Q_{nk}|^2\delta(\omega - E_k) + |Q_{n+1k}|^2\delta(\omega + E_k)].$$

(7)

The SLRR can be written in terms of the spin-spin correlation function as[10]

$$R(i,j) = \lim_{\omega \to 0}\sum_{\alpha,\beta=1}^2\frac{\mathrm{Im}\chi_{\alpha\alpha,\beta\beta}^{-+}(i,j,\omega)}{\omega/T}$$
$$= -\pi T\sum_{o,k=1}^L\sum_{\alpha\beta}Q_{n+1o}Q_{nk}(Q_{mo}^*Q_{m-1k}^* - Q_{m-1o}^*Q_{mk}^*)$$
$$\times f'(E_o)\delta(E_o + E_k). \quad (8)$$

We consider the case $i = j$ by assuming that the nuclear relaxation occurs locally such as on the Fe site. Then the spatially resolved SLRR is given by $T_1^{-1}(i) = R(i,i)$. We note that the SLRR on other atoms like As can be expressed in terms of Eq. (8) with a form factor, which should not change the fundamental physics discussed here. The magnitudes of the parameters are chosen as $t_{1-4} = 1, 0.4, -2, 0.04$. Magnetic unit cells are introduced where each unit cell accommodates two SC flux quanta and the linear dimension is $N_x \times N_y = 64 \times 32$, corresponding to a magnetic field $B \approx 13$ Tesla. V_{ii} and V_{ij} $[i = j \pm (\hat{x} \pm \hat{y})]$ are chosen to be -2.8 and -2, respectively. Throughout the work, we focus on $x = 0.4$, corresponding to the optimally doped compound, and the supercell technique[16] is used to calculate the LDOS and SLRR.

III. RESULTS AND DISCUSSION

First we consider the $s_\pm$ case. For $B = 0$, the $s_\pm$ order parameter is homogeneous in real space. In the presence of an applied magnetic field, our calculations show that the spatial variation of the $s_\pm$ order parameter is similar to that obtained in Ref. 15 (not shown here). Figure 1(a) shows the zero-energy (ZE) LDOS in real space and the position of the sites [V: (16,16), S: (32,16), C: (32,0)] where we calculate $\rho_i(\omega)$ and $T_1^{-1}(i)$. From Fig. 1(b) we can see that at the vortex core center V there is a sharp NE in-gap peak in the LDOS (red dash). By comparing with Ref. 15, we conclude that the existence of this peak is robust since the magnetic field is about $B = 23$ Tesla in Ref. 15. The robustness of the peak has also been verified by STM experiment conducted at magnetic fields of 4 and 9 Tesla.[14] Away from the vortex core center, at the saddle point S and the farthest site C (green dot and blue dash dot, respectively), the LDOS is similar to the $B = 0$ case (black
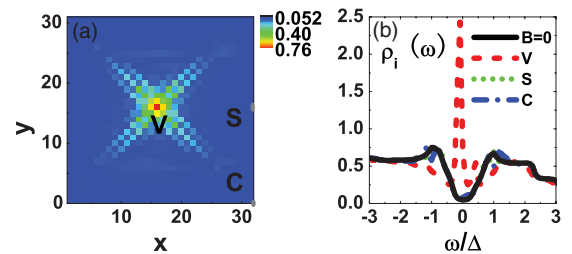

FIG. 1. (Color online) The $s_\pm$ case. (a) The ZE LDOS plotted on a 32×32 lattice and the position of the sites where we calculate $\rho_i(\omega)$ and $T_1^{-1}(i)$. V (vortex core center), S (saddle point), and C (the farthest site) are at sites (16,16), (32,16), and (32,0), respectively. (b) The LDOS as a function of the reduced energy ω/Δ at V (red dash), S (green dot), and C (blue dash dot), as well as that for $B = 0$ (black solid). Here Δ is the zero-field SC gap between two SC coherence peaks in the LDOS.
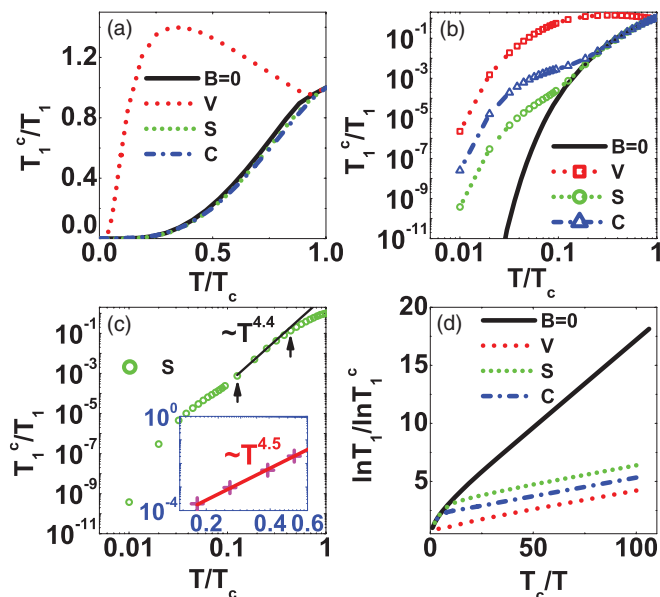
FIG. 2. (Color online) The $s_\pm$ case. (a) $T_1(T_c)/T_1(T)$ as a function of the reduced temperature T/T_c. (b) A log-log plot of (a). (c) Power-law fit of $T_1^{-1}(i)$ at S. T/T_c is from 0.1 to 0.45. (d) $\ln T_1(T)/\ln T_1(T_c)$ as a function of T_c/T. The inset in (c) shows the experimental data taken from Ref. 6 (the magenta cross) and the power-law fit.

solid) with only minor difference in the vicinity of the gap edges.

Then we examine the T dependence of $T_1^{-1}(i)$ at the representative sites shown in Fig. 1(a). We also calculate the zero-field (ZF) case in our formulation for comparison. As pointed out in Sec. I, in an NMR experiment, it is possible to perform the site-selective $T_1^{-1}(i)$ measurement by tuning the RF. The correspondence between the RS and the spatial position of the vortex lattice can be seen from Fig. 1 in Ref. 11. Usually, if the site dependence is not specified, T_1^{-1} is measured at the saddle point S since the RS at S is logarithmically singular (i.e., it has the highest intensity).[17] Thus, T_1^{-1} reported in NMR experiments conducted on the iron pnictides so far[5,6] should correspond to $T_1^{-1}(i)$ measured at S. From Fig. 2(a) we can see that at S, C, and for $B = 0$, there is no coherence peak below T_c. This is considered to be a signature of unconventional superconductivity and is consistent with the experimental observations.[5,6] However, at V, after the initial decrease of $T_1^{-1}(i)$ with the lower temperature, a broad peak below T_c shows up and $T_1^{-1}(i)$ is much larger than that at S and C. From Fig. 2(b) we notice that for $B = 0$, T_1^{-1} indeed does not exhibit the power law but an exponential behavior at low temperature, consistent with previous theories considering $s_\pm$ pairing symmetry in the absence of impurities.[7] In the presence of vortices, $T_1^{-1}(i)$ at S, C, and V deviates drastically from its ZF value, although the LDOS at S and C is similar to that for $B = 0$ [see Fig. 1(b)]. This suggests that $T_1^{-1}(i)$ is not entirely determined by the LDOS as in d-wave superconductors, because in that case, the pairing order parameters on the FS would cancel each other out due to the d-wave symmetry, while in the iron pnictides they cannot do so completely because although the order parameters change sign between the hole and electron pockets, they still have different magnitudes. Furthermore, it is

noted that $T_1^{-1}(i)$ at C is larger than that at S, although C is farther from the vortex center. This is due to the vortex lattice effect: The quasiparticle transfer between vortices occurs along the line connecting NNN vortices (i.e., near C). In Fig. 2(c), we concentrate on $T_1^{-1}(i)$ at S since the available NMR data on the iron pnictides should correspond to that measured at this site. As we can see, for $0.1 \leqslant T/T_c \leqslant 0.45$ (indicated by the two arrows), $T_1^{-1}(i)$ follows a power-law behavior ($\sim T^{4.4}$) that is qualitatively consistent with experiments[6] [see the inset of Fig. 2(c)]. Previously this was considered to indicate that there exist nodes on the FS, ZE quasiparticles induced by impurities or strong anisotropic gaps on the electron pockets.[5–8] However, our results suggest that the mixed-state effect can also lead to the power-law behavior in this temperature range, even if there are no nodes or strong gap anisotropy on the FS, as well as ZE quasiparticles induced by impurities. As the temperature is lowered below $T/T_c \approx 0.1$, $T_1^{-1}(i)$ no longer follows the power law, but an exponential behavior to the lowest temperature considered ($0.01 T_c$), suggesting the opening of full gaps. In principle, only the behavior of T_1 close to zero temperature is considered to be an indication of whether there are nodes or not on the FS. However, the experimental data obtained so far are for temperature above $T/T_c \approx 0.1$, which is not very close to zero. Therefore, the behavior of $T_1^{-1}(i)$ in this temperature range may not truly reflect the pairing symmetry and gap structure. From Fig. 2(d) we can see more clearly that at S, V, C, and for $B = 0$, $T_1^{-1}(i)$ follows the exponential relation below $T/T_c \approx 0.1$. In addition, at low temperature, $T_1(i)$ for $B = 0$ and at V in the mixed state can be fitted as $T_1(i) \sim e^{A/T}$, where $A \approx 0.3\Delta$ and 0.07Δ, respectively. The exponential behavior of $T_1^{-1}(i)$ is similar to that in s-wave superconductors. In Ref. 10, it is suggested that for s-wave pairing, $T_1 \sim e^{\Delta/T}$ for $B = 0$ and $T_1(i) \sim e^{\Delta_1/T}$ at V, where Δ_1 is a small gap between two in-gap peaks at the vortex core center. Apparently, this is not the case in the iron pnictides. From Fig. 1(b) we can see that there is no gap equal to 0.3Δ for $B = 0$ or 0.07Δ at V in the mixed state, again suggesting that in the iron pnictides, $T_1^{-1}(i)$ cannot be entirely determined by the LDOS; the multiorbital physics must be considered.

Next we consider the s-wave case. For $B = 0$, the s-wave order parameter is uniform in real space. Upon applying the magnetic field, the spatial variations of the s-wave order parameter (not shown here) and the ZE LDOS [see Fig. 3(a)] are both similar to the $s_\pm$ case. Furthermore, Figure 3(b) shows that there is also a NE in-gap peak at V whose existence is very similar to the $s_\pm$ case, making the vortex states indistinguishable between the two pairing symmetries. In addition, the LDOS at S and C is again similar to its ZF value. However, $T_1^{-1}(i)$ in the s-wave case is distinctly different. From Fig. 3(c) we notice, right below T_c, a coherence peak shows up at S, C, and for $B = 0$, which is a signature of isotropic s-wave pairing and is in striking contrast to the $s_\pm$ case while at V it behaves similarly to the $s_\pm$ case. For $0.14 \leqslant T/T_c \leqslant 0.43$, $T_1^{-1}(i)$ at S (not shown here) also shows a power-law behavior ($\sim T^7$). Below $T/T_c \approx 0.14$, at S, C, V, and for $B = 0$, $T_1^{-1}(i)$ exhibits an exponential relation [see Fig. 3(d)]. While for $B = 0$, $T_1 \sim e^{A/T}$ with $A \approx \Delta$, A at S and C apparently deviates from Δ, although the LDOS at S and C is similar to that for $B = 0$, which is additional evidence that $T_1^{-1}(i)$ cannot be entirely determined by the LDOS and the mixed-state effect has to be
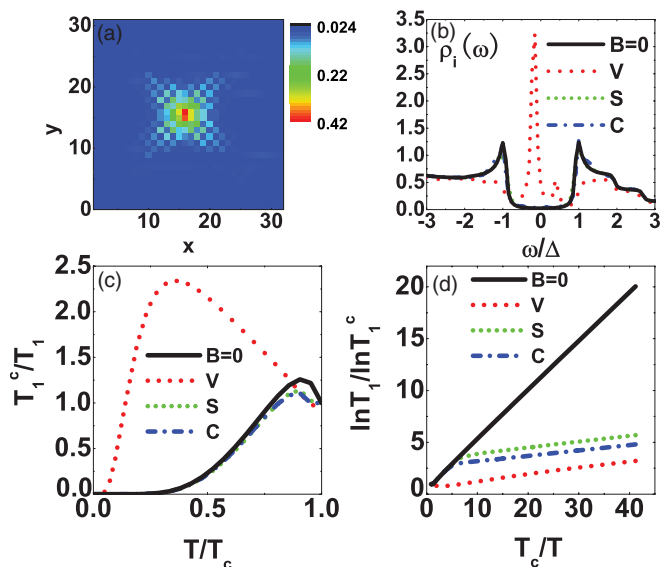
FIG. 3. (Color online) The s-wave case. (a) and (b) are the same as Figs. 1(a) and 1(b), respectively. (c) and (d) are the same as Figs. 2(a) and 2(d), respectively.

considered when comparing theoretical calculations with experimental measurements. Meanwhile, the different behavior of $T_1^{-1}(i)$ at S in the $s_\pm$ and s-wave pairing cases makes it possible to distinguish these two pairing symmetries since the experimentally observed T_1^{-1} shows no coherence peak below T_c, thus excluding the possibility of s-wave pairing.

IV. CONCLUSION

In summary, we have systematically investigated the mixed-state effect on the NMR relaxation rate in the iron pnictides

with $s_\pm$ or s-wave pairing symmetry. For the $s_\pm$ pairing, the SLRR at the saddle point does not exhibit a coherence peak below T_c and shows a power-law behavior from $T/T_c \approx 0.1$–0.45, which is qualitatively consistent with recent NMR experiments. However, at the vortex core center, a broad peak shows up below T_c. On the other hand, for the s-wave pairing, the SLRR at the saddle point shows a coherence peak right below T_c and a power-law behavior from $T/T_c \approx 0.14$–0.43, while at the vortex center, it behaves similarly to the $s_\pm$ case. In both cases, the SLRR follows the exponential relation when approaching $T/T_c \approx 0.01$ down from 0.1, and it cannot be entirely determined by the LDOS. The effect of the magnetic field and multiorbital physics must be considered. Based on the available experimental data, the s-wave pairing can be excluded in the iron pnictides. But in order to clarify whether there are nodes or not, the experiments need to be conducted at even lower temperature.

Note added. Very recently the vortex effects on the SLRR were also studied by using another two-orbital model.[18] Their calculated T_1^{-1} is an average over all the lattice sites and thus may not be relevant to the experiments conducted in the iron pnictides.

[1] Y. Kamihara, T. Watanabe, M. Hirano, and H. Hosono, J. Am. Chem. Soc. **130**, 3296 (2008).

[2] I. I. Mazin, D. J. Singh, M. D. Johannes, and M. H. Du, Phys. Rev. Lett. **101**, 057003 (2008); A. V. Chubukov, M. G. Vavilov, and A. B. Vorontsov, Phys. Rev. B **80**, 140515(R) (2009).

[3] M. Rotter, M. Tegel, and D. Johrendt, Phys. Rev. Lett. **101**, 107006 (2008).

[4] H. Ding, P. Richard, K. Nakayama, K. Sugawara, T. Arakane, Y. Sekiba, A. Takayama, S. Souma, T. Sato, T. Takahashi, Z. Wang, X. Dai, Z. Fang, G. F. Chen, J. L. Luo, and N. L. Wang, Europhys. Lett. **83**, 47001 (2008); K. Nakayama, T. Sato, P. Richard, Y.-M. Xu, Y. Sekiba, S. Souma, G. F. Chen, J. L. Luo, N. L. Wang, H. Ding, and T. Takahashi, *ibid.* **85**, 67002 (2009).

[5] H.-J. Grafe, D. Paar, G. Lang, N. J. Curro, G. Behr, J. Werner, J. Hamann-Borrero, C. Hess, N. Leps, R. Klingeler, and B. Büchner, Phys. Rev. Lett. **101**, 047003 (2008); H. Fukazawa, T. Yamazaki, K. Kondo, Y. Kohori, N. Takeshita, P. M. Shirage, K. Kihou, K. Miyazawa, H. Kito, H. Eisaki, and A. Iyo, J. Phys. Soc. Jpn. **78**, 033704 (2009); H. Nishimura, M. Yashima, H. Mukuda, Y. Kitaoka,

K. Miyazawa, P. M. Shirage, K. Kiho, H. Kito, H. Eisaki, and A. Iyo, Physica C **470**, S466 (2010).

[6] M. Yashima, H. Nishimura, H. Mukuda, Y. Kitaoka, K. Miyazawa, P. M. Shirage, K. Kihou, H. Kito, H. Eisaki, and A. Iyo, J. Phys. Soc. Jpn. **78**, 103702 (2009).

[7] A. V. Chubukov, D. V. Efremov, and I. Eremin, Phys. Rev. B **78**, 134512 (2008); D. Parker, O. V. Dolgov, M. M. Korshunov, A. A. Golubov, and I. I. Mazin, *ibid.* **78**, 134524 (2008); Y. Bang, Han-Yong Choi, and Hyekyung Won, *ibid.* **79**, 054529 (2009).

[8] Y. Nagai, N. Hayashi, N. Nakai, H. Nakamura, M. Okumura, and M. Machida, New J. Phys. **10**, 103026 (2008).

[9] W. Fite II and A. G. Redfield, Phys. Rev. Lett. **17**, 381 (1966).

[10] M. Takigawa, M. Ichioka, and K. Machida, Phys. Rev. Lett. **83**, 3057 (1999).

[11] V. F. Mitrović, E. E. Sigmund, M. Eschrig, H. N. Bachman, W. P. Halperin, A. P. Reyes, P. Kuhns, and W. G. Moulton, Nature (London) **413**, 501 (2001).

[12] Degang Zhang, Phys. Rev. Lett. **103**, 186402 (2009).

[13] C. Liu, G. D. Samolyuk, Y. Lee, N. Ni, T. Kondo, A. F. Santander-Syro, S. L. Bud'ko, J. L. McChesney, E. Rotenberg, T. Valla, A. V. Fedorov, P. C. Canfield, B. N. Harmon, and A. Kaminski,

Phys. Rev. Lett. **101**, 177005 (2008); Y. Sekiba, T. Sato, K. Nakayama, K. Terashima, P. Richard, J. H. Bowen, H. Ding, Y.-M. Xu, L. J. Li, G. H. Cao, Z.-A. Xu, and T. Takahashi, New J. Phys. **11**, 025020 (2009).

[14] L. Shan, Yong-Lei Wang, Bing Shen, Bin Zeng, Yan Huang, Ang Li, Da Wang, Huan Yang, Cong Ren, Qiang-Hua Wang, Shuheng H. Pan, and Hai-Hu Wen, Nature Phys. **7**, 325 (2011).

[15] Y. Gao, Huai-Xiang Huang, Chun Chen, C. S. Ting, and Wu-Pei Su, Phys. Rev. Lett. **106**, 027004 (2011).

[16] Jian-Xin Zhu, B. Friedman, and C. S. Ting, Phys. Rev. B **59**, 3353 (1999).

[17] V. F. Mitrović (private communication).

[18] Hong-Min Jiang, Jia Guo, and Jian-Xin Li, Phys. Rev. B **84**, 014533 (2011).